Communication

Transferrin-Appended Nanocaplet for Transcellular siRNA Delivery into Deep Tissues

Ai Kohata, P.K. Hashim, Kou Okuro, and Takuzo Aida

J. Am. Chem. Soc., **Just Accepted Manuscript** • DOI: 10.1021/jacs.8b12501 • Publication Date (Web): 06 Feb 2019

Transferrin-Appended Nanocaplet for Transcellular siRNA Delivery into Deep Tissues

Ai Kohata,[†] P. K. Hashim,[†] Kou Okuro,*[,†] Takuzo Aida*[,†,‡]

[†]Department of Chemistry and Biotechnology, School of Engineering, The University of Tokyo, 7-3-1 Hongo, Bunkyo-ku, Tokyo 113-8656, Japan

[‡]Riken Center for Emergent Matter Science, 2-1 Hirosawa, Wako, Saitama 351-0198, Japan

Supporting Information Placeholder

ABSTRACT: Transferrin (Tf) is known to induce transcytosis, which is a consecutive endocytosis/exocytosis event. We developed a Tf-appended nanocaplet (^{Tf}NC⊃siRNA) for the purpose of realizing siRNA delivery into deep tissues and RNA interference (RNAi) subsequently. For obtaining ^{Tf}NC⊃siRNA, a macromonomer (^{Az}Gu) bearing multiple guanidinium (Gu^+) ion units, azide (N_3) groups, and trityl (Trt)-protected thiol groups in the main chain, side chains, and termini, respectively, was newly designed. Because of a multivalent Gu^+–phosphate salt-bridge interaction, ^{Az}Gu can adhere to siRNA along its strand. When I_2 was added to a preincubated mixture of ^{Az}Gu and siRNA, oxidative polymerization of ^{Az}Gu took place along the siRNA strand, affording ^{Az}NC⊃siRNA, the smallest siRNA-containing reactive nanocaplet so far reported. This conjugate was converted into $^{Glue/BP}$NC⊃siRNA by the click reaction with a Gu^+-appended bio-adhesive dendron (Glue) followed by a benzophenone derivative (BP). Then, Tf was covalently immobilized onto $^{Glue/BP}$NC⊃siRNA by Gu^+-mediated adhesion followed by photochemical reaction with BP. With the help of Tf-induced transcytosis, ^{Tf}NC⊃siRNA permeated deeply into a cancer spheroid, a 3D-tissue model, at depth of up to nearly 70 μm, unprecedentedly.

Tissue-permeable nanocarriers for small interfering RNA (siRNA) are essential for the realization of RNA interference (RNAi)-based gene therapy[1] for diseases that develop in deep tissues at depth of >40 μm from the vascular endothelium.[2] For instance, metastatic cancers often spread over tissues at depth of up to ~300 μm from blood vessels.[3] For the tissue permeation of nanocarriers, paracellular and transcellular pathways are considered.[4] However, paracellular siRNA delivery is unlikely since intercellular gaps (5–10 nm)[5] are not large enough for siRNA (~5 nm)[6] to pass through. For the purpose of achieving transcellular delivery of siRNA into deep tissues, the carrier is preferred to be as small as possible[7] and needs to be reductively cleavable in cytoplasm. Furthermore, it should be active for transcytosis (consecutive endocytosis/exocytosis events). Although a few carriers that bear particular ligands for activating transcytosis such as transferrin (Tf),[8] Tf-receptor binding peptides,[9] and RGD peptides[10] have been reported, successful examples of siRNA delivery feature the best delivery depth of only 20–40 μm,[9a,10a] most likely due to their large dimensions. Namely, siRNA delivery into tissues deeper than 40 μm still remains a big challenge.

Herein, we report a siRNA-containing nanocaplet appended with Tf units (^{Tf}NC⊃siRNA, Figure 1e), which can deeply deliver siRNA into tissues at depth of up to nearly 70 μm, unprecedentedly (Figure 2). Prior to the present work, we developed water-soluble molecular glues[11] bearing multiple guanidinium (Gu^+) ion units that can strongly adhere to proteins,[12] nucleic acids,[13] phospholipid membranes,[14] and even clay nanosheets[15] through multiple salt-bridge interactions with their oxyanionic functionalities.[16] We found that a siRNA strand can template oxidative polymerization of a Gu^+-appended telechelic macromonomer carrying four Gu^+ units as well as thiol (SH) termini, affording a siRNA-containing nanocaplet NC (NC⊃siRNA) with a hydrodynamic diameter (D_h) of <10 nm.[13a] NC is the smallest nanocaplet for siRNA so far reported. The disulfide (SS) bonds forming the NC part are readily cleaved off under reductive conditions.[17] Hence, in cytoplasm that contains glutathione (GSH) abundantly (Figure 1d), NC⊃siRNA is possibly disrupted to liberate siRNA that causes RNAi.[13a] We envisioned that its Tf-appended version (^{Tf}NC⊃siRNA) may deliver siRNA into deep tissues.[18] In the present study, we synthesized a siRNA-containing reactive nanocaplet ^{Az}NC⊃siRNA (Figure 1e) by oxidative polymerization of ^{Az}Gu, an azide (N_3)-appended telechelic macromonomer (Figure 1a). Then, ^{Az}NC⊃siRNA was allowed to react with a Gu^+-appended bioadhesive dendron (Glue-alkyne) followed by a benzophenone (BP) deriv-

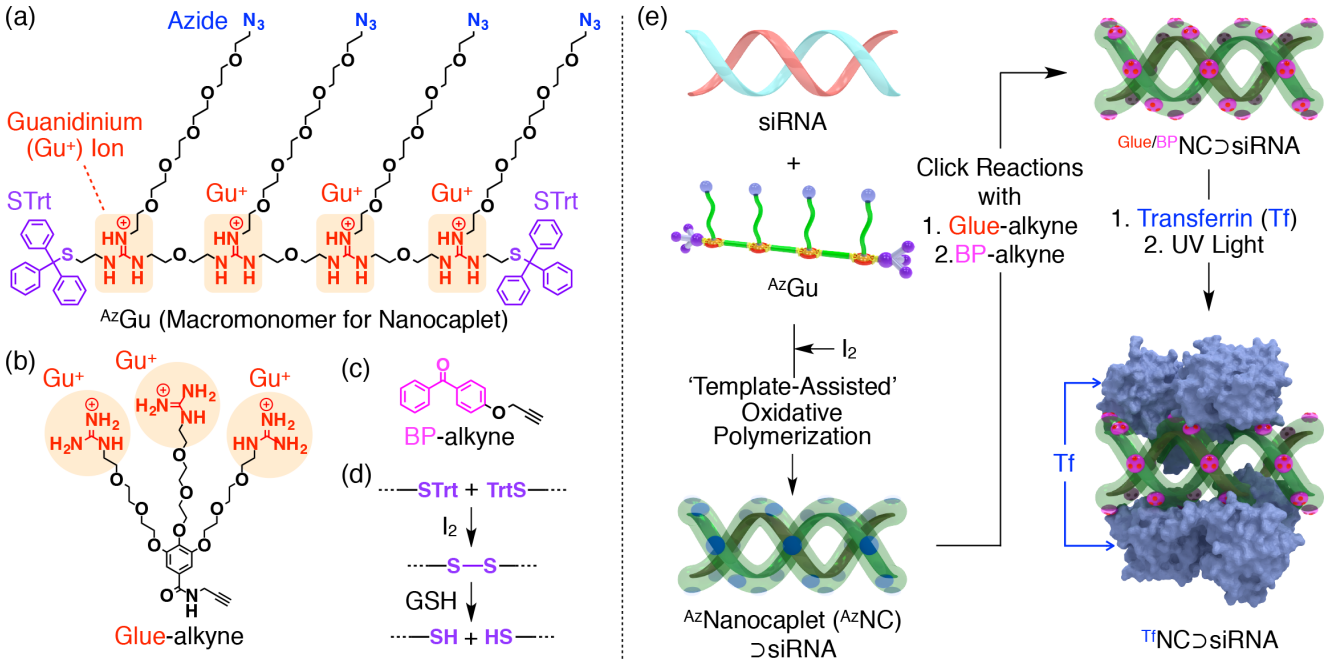

Figure 1. Molecular structures of (a) ^{Az}Gu, an azide (N_3)-appended telechelic macromonomer bearing guanidinium (Gu^+) ions and trityl (Trt)-protected thiol (STrt) termini, (b) Glue-alkyne bearing Gu^+-appended dendron (Glue) and an alkyne group at the focal core, and (c) BP-alkyne (alkyne-appended benzophenone). (d) Iodine (I_2)-mediated disulfide formation between Trt-protected thiols and reductive cleavage of a disulfide bond into thiols by glutathione (GSH). (e) Synthesis of a siRNA-containing nanocaplet appended with transferrin (Tf) units (^{Tf}NC⊃siRNA): ^{Az}Gu is oxidatively polymerized using siRNA as a template to yield a siRNA-containing N_3-appended nanocaplet (^{Az}NC⊃siRNA). Then, Glue-alkyne and BP-alkyne are allowed to react successively with ^{Az}NC⊃siRNA (click reactions) to yield $^{Glue/BP}$NC⊃siRNA. At the initial stage, Tf is noncovalently attached to the surface of $^{Glue/BP}$NC⊃siRNA through a multivalent salt-bridge interaction with the dendritic Gu^+ pendants and then immobilized covalently by a photochemical reaction with BPs.

ative (BP-alkyne) to obtain $^{Glue/BP}$NC⊃siRNA (Figure 1e). Subsequently, this conjugate was incubated with Tf, and the mixture was exposed to UV light for covalent immobilization of the attached Tf units by reacting with the BP units, affording ^{Tf}NC⊃siRNA (Figure 1e). As highlighted in this communication, ^{Tf}NC⊃siRNA deeply permeated into a cancer spheroid, a 3D tissue model, at depth of up to nearly 70 μm. This unprecedented achievement possibly takes advantage of the small dimensional aspect of ^{Tf}NC⊃siRNA and its transcytosis activity mediated by the surface Tf units.

^{Az}Gu, Glue-alkyne, and BP-alkyne (Figures 1a–c) were synthesized according to the procedures described in the Supporting Information and characterized unambiguously using a variety of analytical methods.[19] ^{Az}NC⊃siRNA (Figure 1e) was prepared in the presence of siRNA by deprotection of the Trt groups of ^{Az}Gu using I_2 and subsequent oxidative polymerization of the deprotected macromonomer (Figure 1d). $^{Glue/BP}$NC⊃siRNA was obtained by the copper-catalyzed successive 'click' reactions of Glue-alkyne (Figure 1b) and BP-alkyne (Figure 1c) with the azide groups of ^{Az}NC⊃siRNA (Figure 1e), where the ratio of $Gu^+/BP/N_3$ in $^{Glue/BP}$NC⊃siRNA was estimated as 23/5/22 by MALDI-TOF mass spectrometry (Figure S5)[19] after the reductive depolymerization of $^{Glue/BP}$NC⊃siRNA using dithiothreitol (DTT).

^{Tf}NC⊃siRNA was successfully obtained by 10-min UV irradiation (λ = 310 nm) of a mixture of $^{Glue/BP}$NC⊃siRNA ([siRNA] = 0.2 μM) and Tf (1.1 μM; Figure 1e). Dynamic light scattering (DLS) analysis indicated that ^{Tf}NC⊃siRNA has a D_h value of 15.8 ± 5.0 nm (Figure 3c, blue), which is reasonable considering that the D_h values of $^{Glue/BP}$NC⊃siRNA and Tf are 6.1 ± 0.7 nm (Figure 3c, red) and 7.1 ± 0.2 nm (Figure S6),[19] respectively. Accordingly, cryogenic transmission electron microscopy (cryo-TEM) allowed for visualizing ^{Tf}NC⊃siRNA as spherical objects with a diameter of ~20 nm (Figure 3d). For the purpose of characterizing its charge density by means of agarose gel electrophoresis, we carried out the above reaction (Figure 1e, right) using rhodamine-attached fluorescent Tf (^{Rhd}Tf). As shown in Figure 3a (right), ^{Tf}NC⊃siRNA migrated toward a negative electrode side, whereas, in the absence (Figure 3a, left) and presence (Figure 3a, center) of $^{Glue/BP}$NC⊃siRNA, negatively charged ^{Rhd}Tf migrated toward a positive electrode side. Accordingly, ^{Tf}NC⊃siRNA displayed a positive zeta-

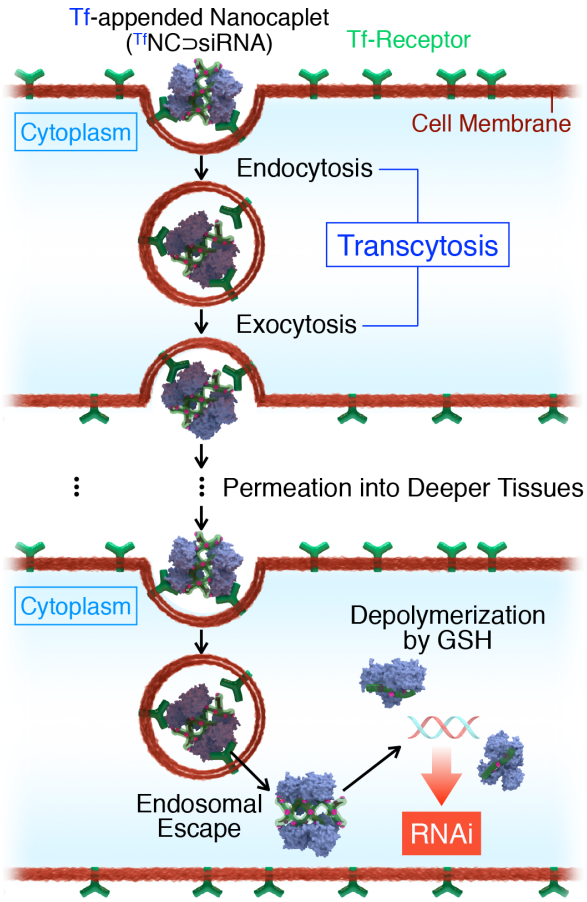

Figure 2. Permeation of ^{Tf}NC⊃siRNA into cells located in a deep tissue via Tf-mediated transcytosis. Once ^{Tf}NC⊃siRNA escapes from the endosomes in a cell, glutathione (GSH), abundantly present in the cytoplasm, liberates siRNA to cause RNAi by reductive depolymerization of the nanocaplet part (^{Tf}NC).

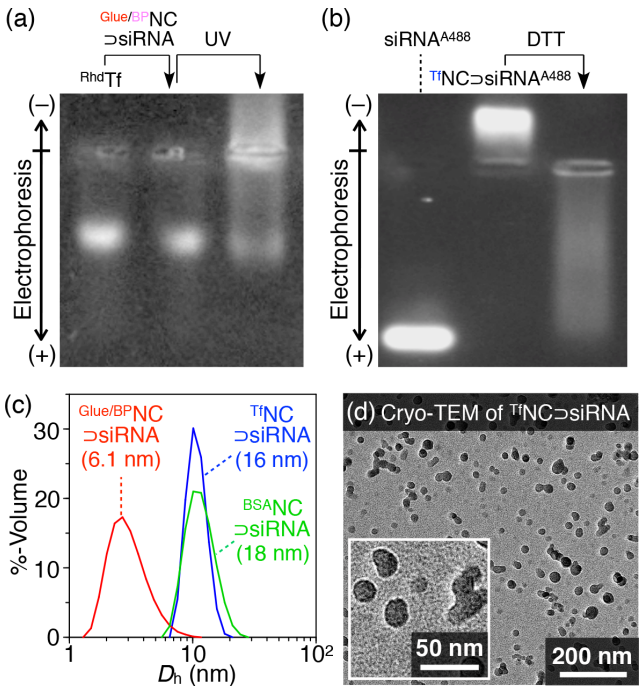

Figure 3. (a) Agarose gel electrophoretic profiles (λ_{ext} = 495 nm) of rhodamine-attached fluorescent Tf (^{Rhd}Tf, 1.1 μM) before and after being mixed with $^{Glue/BP}$NC⊃siRNA ([siRNA] = 0.2 μM), followed by 10-min photoirradiation at 310 nm. (b) Agarose gel electrophoretic profiles (λ_{ext} = 495 nm) of siRNA fluorescently labeled with Alexa Fluor 488 (siRNA^{A488}, 0.5 μM) and ^{Tf}NC⊃siRNA^{A488} ([siRNA^{A488}] = 0.5 μM) before and after 1-h incubation at 25 °C in the presence of dithiothreitol (DTT, 10 mM). (c) Dynamic light scattering histograms in HEPES buffer (20 mM, pH 7.3) at 25 °C of $^{Glue/BP}$NC⊃siRNA ([siRNA] = 2 μM, red), ^{Tf}NC⊃siRNA ([siRNA] = 2 μM, blue) and ^{BSA}NC⊃siRNA ([siRNA] = 2 μM, green). (d) A cryogenic transmission electron microscopy (cryo-TEM) image of a HEPES buffer (20 mM, pH 7.0) solution of ^{Tf}NC⊃siRNA ([siRNA] = 3 μM). Inset: a magnified image of (d).

potential (ζ) of 5 ± 2 mV (Table S1).[19] ^{Tf}NC⊃siRNA^{A488} incorporating Alexa Fluor 488-labeled siRNA (siRNA^{A488}; 1 μM) displayed the same electrophoretic tendency as ^{Tf}NC⊃siRNA (Figure 3b, center). As described above, the SS bonds in NC are readily cleaved off in a reductive environment. In fact, when ^{Tf}NC⊃siRNA^{A488} was incubated with DTT (10 mM) for 1 h at 25 °C in HEPES buffer, the electrophoretic profile of the reaction mixture became broadened toward a positive electrode side (Figure 3b, right), indicating the occurrence of reductive breakdown of the ^{Tf}NC part (Figure S8).[19]

^{Tf}NC⊃siRNA enters living cells via endocytosis: Human hepatocellular carcinoma Hep3B cells (1.0×10^4 cells/well) were incubated for 4 h at 37 °C in a serum-free minimal essential medium (MEM, 200 μL) containing ^{Tf}NC⊃siRNA^{A488} ([siRNA^{A488}] = 50 nM). Then, the sample was rinsed with Dulbecco's phosphate buffered saline (D-PBS, 100 μL × 2), and subjected to confocal laser scanning microscopy (CLSM; λ_{ext} = 488 nm). As shown in Figure 4a, the cells became fluorescent, indicating the incorporation of fluorescently labeled siRNA^{A488} into the cells, whereas the cells incubated with ^{Az}NC⊃siRNA^{A488} (Figure 4c) or naked siRNA^{A488} (Figure 4d) ([siRNA^{A488}] = 50 nM) did not fluoresce. When the Tf units in ^{Tf}NC⊃siRNA^{A488} were replaced with bovine serum albumin (BSA; ^{BSA}NC⊃siRNA^{A488}), the fluorescence emission from Hep3B cells was again negligibly weak (Figure 4b), although ^{BSA}NC⊃siRNA has a comparable size (D_h = 18.2 ± 0.3 nm; Figure 3c, green) and surface charges (ζ = 3 ± 0.4 mV; Table S1)[19] to those of ^{Tf}NC⊃siRNA (D_h = 15.8 ± 5.0 nm and ζ = 5 ± 2 mV; Figure 3c, blue and Table S1, respectively).[19] It should be noted that at 4 °C, where endocytosis is known to be suppressed,[20] Hep3B cells barely took up ^{Tf}NC⊃siRNA^{A488} (Figure S7).[19] Hence, the cellular uptake of

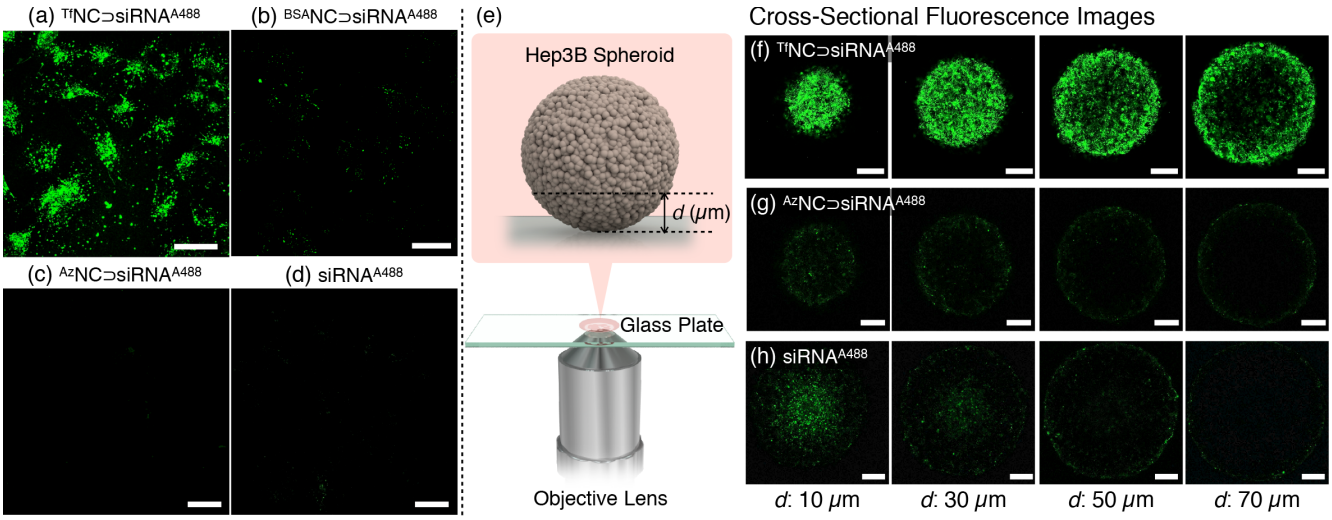

Figure 4. (a–d) Confocal laser scanning microscopy (CLSM; λ_{ext} = 488 nm, λ_{obs} = 510–590 nm) images of Hep3B cells after a 4-h incubation at 37 °C in MEM with (a) ^{Tf}NC⊃siRNA^{A488} ([siRNA^{A488}] = 50 nM), (b) ^{BSA}NC⊃siRNA^{A488} ([siRNA^{A488}] = 50 nM), (c) ^{Az}NC⊃siRNA^{A488} ([siRNA^{A488}] = 50 nM), and (d) siRNA^{A488} ([siRNA^{A488}] = 50 nM). Scale bars = 25 μm. (e) Schematic illustration of the experimental setup for obtaining cross-sectional CLSM images of a Hep3B spheroid. (f–g) Cross-sectional CLSM (λ_{ext} = 488 nm, λ_{obs} = 510–590 nm) images of Hep3B spheroids at depth of 10, 30, 50, and 70 μm from the surface after a 3-day incubation at 37 °C in MEM (10% FBS) in the presence of (f) ^{Tf}NC⊃siRNA^{A488} ([siRNA^{A488}] = 100 nM), (g) ^{Az}NC⊃siRNA^{A488} ([siRNA^{A488}] = 100 nM), and (h) siRNA^{A488} (100 nM). Scale bars = 100 μm.

^{Tf}NC⊃siRNA occurs most likely via endocytosis, and this process is mediated by the Tf units in ^{Tf}NC⊃siRNA.

The above observations prompted us to investigate whether ^{Tf}NC⊃siRNA indeed activates transcytosis or not. For this purpose, we prepared a 3D-cultured Hep3B spheroid with an average diameter of ~500 μm (Figure 4e) by using 96-well cell-repellent plates,[19] and incubated with ^{Tf}NC⊃siRNA^{A488} ([siRNA^{A488}] = 100 nM) in MEM (100 μL, 10% FBS) for 3 days at 37 °C. After being rinsed with D-PBS buffer (100 μL × 2), the resultant spheroid was subjected to CLSM (λ_{ext} = 488 nm). Fortunately, we found that the spheroid fluoresced throughout its cross sections at depth of 10, 30, and 50 μm (Figure 4f). Notably, even at depth of 70 μm, ^{Tf}NC⊃siRNA^{A488} reached the central part of the cross section (Figure 4f), indicating the deep permeation of ^{Tf}NC⊃siRNA^{A488}. In sharp contrast, the spheroid barely fluoresced when incubated with ^{Az}NC⊃siRNA^{A488} (Figure 4g) and siRNA^{A488} (Figure 4h) ([siRNA^{A488}] = 100 nM), in consistency with their poor cellular uptake behaviors (Figures 4c and 4d, respectively). All these observations indicate that ^{Tf}NC⊃siRNA activates transcytosis.

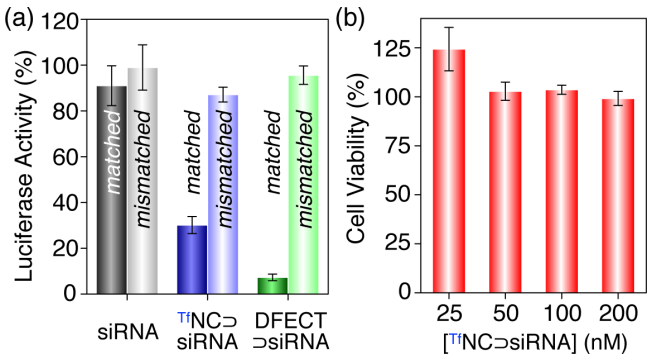

Figure 5. (a) Normalized luciferase activities of Hep3B-luc cells using the PicaGene LT 2.0 luciferase assay kit. Here, Hep3B-luc cells were incubated at 37 °C for 72 h in MEM (10% FBS) in the presence of siRNA (50 nM, black bar), siRNA^{mis} (50 nM, gray bar), ^{Tf}NC⊃siRNA ([siRNA or siRNA^{mis}] = 50 nM; siRNA and siRNA^{mis}, purple and light purple bars, respectively), and DFECT⊃siRNA ([siRNA or siRNA^{mis}] = 50 nM; siRNA and siRNA^{mis}, green and light green bars, respectively). (b) Normalized cell viabilities of Hep3B cells using Cell Counting Kit-8. Hep3B cells were incubated at 37 °C for 24 h in MEM (10% FBS) in the presence of ^{Tf}NC⊃siRNA ([siRNA] = 25, 50, 100, and 200 nM).

^{Tf}NC⊃siRNA successfully induced RNAi to suppress the expression of a target gene. Thus, mutant Hep3B cells stably expressing luciferase (Hep3B-luc) were incubated for 72 h at 37 °C in MEM (10% FBS) containing ^{Tf}NC⊃siRNA ([siRNA] = 50 nM). Then, the sample was subjected to the luciferase activity assay using PicaGene LT 2.0 as a luminescence reagent (TOYO INK). As shown in Figure 5a, the cells incubated with ^{Tf}NC⊃siRNA exhibited a much lower luciferase activity (purple bar, 30%) than the reference cells incubated with naked siRNA (black bar). Similarly, siRNA conjugated with DharmaFECT 1 (DFECT), a commercially available transfection agent, suppressed the luciferase activity as expected (Figure 5a, green bar, 7%). As a control, ^{Tf}NC⊃siRNA^{mis}, obtained with mismatched siRNA (siRNA^{mis}) that is incapable of inducing RNAi for the luciferase

gene, was used instead of ^{Tf}NC⊃siRNA for the above experiment. As shown in Figure 5a, the luciferase activity of Hep3B-luc cells remained substantially unchanged (light purple bar, 87%). Hence, the decrease in the luciferase activity observed in Figure 5a (purple bar) indicates the occurrence of RNAi. Fortunately, ^{Tf}NC⊃siRNA did not show any appreciable cytotoxicity with its concentration up to 200 nM (Figure 5b).

In conclusion, we developed a transferrin (Tf)-appended siRNA nanocaplet (^{Tf}NC⊃siRNA) capable of delivering siRNA into deep tissues at depth of up to ~70 μm. As demonstrated with a cancer spheroid, ^{Tf}NC⊃siRNA permeates into deep areas of tissues via transcytosis (Figure 2). ^{Tf}NC⊃siRNA eventually transfers siRNA into cytoplasm and causes RNAi and gene knockdown (Figure 2). Because brain endothelial cells are known to express high level of Tf-receptors,[21] ^{Tf}NC⊃siRNA has the potential for overcoming the blood-brain barrier (BBB). Thus, an *in vivo* study on siRNA delivery to brain tissues using ^{Tf}NC⊃siRNA is a subject worthy of further investigation.

ASSOCIATED CONTENT

The Supporting Information is available free of charge on the ACS Publications website.
Synthesis of ^{Az}Gu, Glue-alkyne, and BP-alkyne; ^{1}H NMR, ^{13}C NMR, and MALDI-TOF-MS spectral data; and related experimental procedures (PDF)

AUTHOR INFORMATION

Corresponding Authors

okuro@macro.t.u-tokyo.ac.jp; aida@macro.t.u-tokyo.ac.jp

Notes

The authors declare no competing financial interest.

ACKNOWLEDGMENTS

This work was supported by JSPS KAKENHI Early-Career Scientists (18K14353 and 18K14270) to K.O. and P.K.H., respectively, and partially supported by Grant-in-Aid for Scientific Research (S) (18H05260) to T.A. A.K. thanks JSPS for the world-leading innovative graduate study program for life science and technology (WINGS-LST). We appreciate Prof. H. Cabral and Dr. Y. Anraku (the University of Tokyo) for zeta-potential measurements and fruitful discussions on transcytosis assays using cancer spheroids.

REFERENCES

(1) (a) Hannon, G. J. RNA Interference. *Nature* **2002**, *418*, 244. (b) Bumcrot, D.; Manoharan, M.; Koteliansky, V.; Sah, D. W. Y. RNAi Therapeutics: A Potential New Class of Pharmaceutical Drugs. *Nat. Chem. Biol.* **2006**, *2*, 711. (c) Kim, D. H.; Rossi, J. J. Strategies for Silencing Human Disease using RNA Interference. *Nat. Rev. Genet.* **2007**, *8*, 173.

(2) (a) Trédan, O.; Galmarini, C. M.; Patel, K.; Tannock I. F. Drug Resistance and the Solid Tumor Microenvironment. *J. Natl. Cancer Inst.* **2007**, *99*, 1441. (b) Kim, H. J.; Kim, A.; Miyata, K.; Kataoka, K. Recent Progress in Development of siRNA Delivery Vehicles for Cancer Therapy. *Adv. Drug Delivery Rev.* **2016**, *104*, 61.

(3) Nacev, A.; Kim, S. H.; Rodoriguez-Canales, J.; Tangrea, M. A.; Shapiro, B.; Emmert-Buck, M. R. A Dynamic Magnetic Shift Method to Increase Nanoparticle Concentration in Cancer Metastases: A Feasibility Study Using Simulations on Autopsy Specimens. *Int. J. Nanomed.* **2011**, *6*, 2907.

(4) (a) Tuma, P. L.; Hubbard, A. L. Transcytosis: Crossing Cellular Barriers. *Physiol. Rev.* **2003**, *83*, 871. (b) Zheng, M.; Tao, W.; Zou, Y.; Farokhzad, O. C.; Shi, B. Nanotechnology-Based Strategies for siRNA Brain Delivery for Disease Therapy. *Trends Biotechnol.* **2018**, *36*, 562.

(5) (a) Friend, D. S.; Gilula, N. B. Variations in Tight and Gap Junctions in Mammalian Tissues. *J. Cell Biol.* **1972**, *53*, 758. (b) Itallie, C. M. V.; Anderson, J. M. Claudins and Epithelial Paracellular Transport. *Annu. Rev. Physiol.* **2006**, *68*, 403.

(6) Law, M.; Jafari, M.; Chen, P. Physicochemical Characterization of siRNA-Peptide Complexes. *Biotechnol. Prog.* **2008**, *24*, 957.

(7) (a) Akinc, A.; Battaglia, G. Exploiting Endocytosis for Nanomedicines. *Cold Spring Harbor Perspect. Biol.* **2013**, *5*, a016980. (b) Lu, W.; Xiong, C.; Zhang, R.; Shi, L.; Huang, M.; Zhang, G.; Song, S.; Huang, Q.; Liu, G.; Li, C. Receptor-Mediated Transcytosis: A Mechanism for Active Extravascular Transport of Nanoparticles in Solid Tumors. *J. Controlled Release* **2012**, *161*, 959.

(8) (a) Sarisozen, C.; Abouzeid, A. H.; Torchilin, V. P. The Effect of Co-delivery of Paclitaxel and Curcumin by Transferrin-Targeted PEG-PE-Based Mixed Micelles on Resistant Ovarian Cancer in 3-D Spheroids and *in vivo* Tumors. *Eur. J. Pharm. Biopharm.* **2014**, *88*, 539. (b) Liu, T.; Kempson, I.; Jonge, M.; Howard, D. L.; Thierry, B. Quantitative Synchrotron X-ray Fluorescence Study of the Penetration of Transferrin-Conjugated Gold Nanoparticles inside Model Tumour Tissues. *Nanoscale* **2014**, *6*, 9774.

(9) (a) Wei, L.; Guo, X.; Yang, T.; Yu, M.; Chen, D.; Wang, J. Brain Tumor-Targeted Therapy by Systemic Delivery of siRNA with Transferrin Receptor-Mediated Core-Shell Nanoparticles. *Int. J. Pharm.* **2016**, *510*, 394. (b) Youn, P.; Chen, Y.; Furgeson, D. Y. A Myristoylated Cell-Penetrating Peptide Bearing a Transferrin Receptor-Targeting Sequence for Neuro-Targeted siRNA Delivery. *Mol. Pharmaceutics* **2014**, *11*, 486.

(10) (a) Waite, C. L.; Roth, C. M. PAMAM-RGD Conjugates Enhance siRNA Delivery Through a Multicellular Spheroid Model of Malignant Glioma. *Bioconjugate Chem.* **2009**, *20*, 1908. (b) Jiang, X.; Xin, H.; Gu, J.; Xu, X.; Xia, W.; Chen, S.; Xie, Y.; Chen, L.; Chen, Y.; Sha, X.; Fang, X. Solid Tumor Penetration by Integrin-Mediated Pegylated Poly(trimethylene carbonate) Nanoparticles Loaded with Paclitaxel. *Biomaterials* **2013**, *34*, 1739. (c) Liu, X.; Lin, P.; Perrett, I.; Lin, J.; Liao, Y.; Chang, C. H.; Jiang, J.; Wu, N.; Donahue, T.; Wainberg, Z.; Nel, A. E.; Meng, H. Tumor-Penetrating Peptide Enhances Transcytosis of Silicasome-Based Chemotherapy for Pancreatic Cancer. *J. Clin. Invest.* **2017**, *127*, 2007.

(11) Mogaki, R.; Hashim, P. K.; Okuro, K.; Aida, T. Guanidinium-Based "Molecular Glues" for Modulation of Biomolecular Functions. *Chem. Soc. Rev.* **2017**, *46*, 6480.

(12) (a) Okuro, K.; Kinbara, K.; Tsumoto, K.; Ishii, N.; Aida, T. Molecular Glues Carrying Multiple Guanidinium Ion Pendants via an Oligoether Spacer: Stabilization of Microtubules against Depolymerization. *J. Am. Chem. Soc.* **2009**, *131*, 1626. (b) Okuro, K.; Kinbara, K.; Takeda, K.; Inoue, Y.; Ishijima, A.; Aida, T. Adhesion Effects of a Guanidinium Ion Appended Dendritic "Molecular Glue" on the ATP-Driven Sliding Motion of Actomyosin. *Angew. Chem., Int. Ed.* **2010**, *49*, 3030. (c) Uchida, N.; Okuro, K.; Niitani, Y.; Ling, X.; Ariga, T.; Tomishige, M.; Aida, T. Photoclickable Dendritic Molecular Glue: Noncovalent-to-Covalent Photochemical Transformation of Protein Hybrids. *J. Am. Chem. Soc.* **2013**, *135*, 4684. (d) Garzoni, M.; Okuro, K.; Ishii, N.; Aida, T.; Pavan, G. M. Structure and Shape Effects of Molecular Glue on Supramolecular Tubulin Assemblies. *ACS Nano* **2014**, *8*, 904. (e) Mogaki, R.; Okuro, K.; Aida, T. Molecular Glues for Manipulating Enzymes: Trypsin Inhibition by Benzamidine-Conjugated Molecular Glues. *Chem. Sci.* **2015**, *6*, 2802. (f) Okuro, K.; Sasaki, M.; Aida, T. Boronic Acid-Appended Molecular Glues for ATP-Responsive Activity Modulation of Enzymes. *J. Am. Chem. Soc.* **2016**, *138*, 5527. (g) Mogaki, R.; Okuro, K.; Aida, T. Adhesive Photoswitch: Selective Photochemical Modu-

lation of Enzymes under Physiological Conditions. *J. Am. Chem. Soc.* **2017**, *139*, 10072.

(13) (a) Hashim, P. K.; Okuro, K.; Sasaki, S.; Hoashi, Y.; Aida, T. Reductively Cleavable Nanocaplets for siRNA Delivery by Template-Assisted Oxidative Polymerization. *J. Am. Chem. Soc.* **2015**, *137*, 15608. (b) Hatano, J.; Okuro, K.; Aida, T. Photoinduced Bioorthogonal 1,3-Dipolar Polycycloaddition Promoted by Oxyanionic Substrates for Spatiotemporal Operation of Molecular Glues. *Angew. Chem., Int. Ed.* **2016**, *55*, 193. (c) Okuro, K.; Nemoto, H.; Mogaki, R.; Aida, T. Dendritic Molecular Glues with Reductively Cleavable Guanidinium Ion Pendants: Highly Efficient Intracellular siRNA Delivery via Direct Translocation. *Chem. Lett.* **2018**, *47*, 1232.

(14) (a) Suzuki, Y.; Okuro, K.; Takeuchi, T.; Aida, T. Friction-Mediated Dynamic Disordering of Phospholipid Membrane by Mechanical Motions of Photoresponsive Molecular Glue: Activation of Ion Permeation. *J. Am. Chem. Soc.* **2012**, *134*, 15273. (b) Arisaka, A.; Mogaki, R.; Okuro, K.; Aida, T. Caged Molecular Glues as Photoactivatable Tags for Nuclear Translocation of Guests in Living Cells. *J. Am. Chem. Soc.* **2018**, *140*, 2687.

(15) (a) Wang, Q.; Mynar, J. L.; Yoshida, M.; Lee, E.; Lee, M.; Okuro, K.; Kinbara, K.; Aida, T. High-Water-Content Mouldable Hydrogels by Mixing Clay and a Dendritic Molecular Binder. *Nature* **2010**, *463*, 339. (b) Tamesue, S.; Ohtani, M.; Yamada, K.; Ishida, Y.; Spruell, J. M.; Lynd, N. A.; Hawker, C. J.; Aida, T. Linear versus Dendritic Molecular Binders for Hydrogel Network Formation with Clay Nanosheets: Studies with ABA Triblock Copolyethers Carrying Guanidinium Ion Pendants. *J. Am. Chem. Soc.* **2013**, *135*, 15650.

(16) Sakai, N.; Matile, S. Anion-Mediated Transfer of Polyarginine across Liquid and Bilayer Membranes. *J. Am. Chem. Soc.* **2003**, *125*, 14348.

(17) (a) Bang, E.-K.; Lista, M.; Sforazzini, G.; Sakai, N.; Matile, S. Poly(disulfide)s. *Chem. Sci.* **2012**, *3*, 1752. (b) Bang, E.-K.; Gasparini, G.; Molinard, G.; Roux, A.; Sakai, N.; Matile, S. Substrate-Initiated Synthesis of Cell-Penetrating Poly(disulfide)s. *J. Am. Chem. Soc.* **2013**, *135*, 15650. (c) Bang, E.-K.; Ward, S.; Gasparini, G.; Sakai, N.; Matile, S. Cell-Penetrating Poly(disulfide)s: Focus on Substrate-Initiated Co-polymerization. *Polym. Chem.* **2014**, *5*, 2433. (d)Gasparini, G.; Bang, E.-K.; Molinard, G.; Tulumello, D. V.; Ward, S.; Kelley, S. O.; Roux, A.; Sakai, N.; Matile, S. Cellular Uptake of Substrate-Initiated Cell-Penetrating Poly(disulfide)s. *J. Am. Chem. Soc.* **2014**, *136*, 6069. (e) Chuard, N.; Gasparini, G.; Roux, A.; Sakai, N.; Matile, S. Cell-penetrating Poly(disulfide)s: The Dependence of Activity, Depolymerization Kinetics and Intracellular Localization on Their Length. *Org. Biomol. Chem.* **2015**, *13*, 64. (f) Gasparini, G.; Matile, S. Protein Delivery with Cell-Penetrating Poly(disulfide)s. *Chem. Commun.* **2015**, *51*, 17160. (g) Morelli, P.; Martin-Benlloch, X.; Tessier, R.; Waser, J.; Sakai, N.; Matile, S. Ethynyl Benziodoxolones: Functional Terminators for Cell-Penetrating Poly(disulfide)s. *Polym. Chem.* **2016**, *7*, 3465. (h) Morelli, P.; Matile, S. Sidechain Engineering in Cell-Penetrating Poly(disulfide)s. *Helv. Chim. Acta* **2017**, *100*, e1600370. (i) Derivery, E.; Bartolami, E.; Matile, S.; Gonzalez-Gaitan, M. Efficient Delivery of Quantum Dots into the Cytosol of Cells Using Cell-Penetrating Poly(disulfide)s. *J. Am. Chem. Soc.* **2017**, *139*, 10172. (j) Morelli, P.; Bartolami, E.; Sakai, N.; Matile, S. Glycosylated Cell-Penetrating Poly(disulfide)s: Multifunctional Cellular Uptake at High Solubility. *Helv. Chim. Acta* **2018**, *101*, e1700266.

(18) Chithrani, B. D.; Chan, W. C. W. Elucidating the Mechanism of Cellular Uptake and Removal of Protein-Coated Gold Nanoparticles of Different Sizes and Shapes. *Nano Lett.* **2007**, *7*, 1542.

(19) See Supporting Information.

(20) Casley-Smith, J. R. Endocytosis: The Different Energy Requirements for the Uptake of Particles by Small and Large Vesicles into Peritoneal Macrophages. *J. Microsc.* **1969**, *90*, 15.

(21) (a) Jefferies, W. A.; Brandon, M. R.; Hunt, S. V.; Williams, A. F.; Gatter, K. C.; Mason, D. Y. Transferrin Receptor on Endothelium of Brain Capillaries. *Nature* **1984**, *312*, 162. (b) Qian, Z. M.; Li, H.; Sun, H.; Ho, K. Targeted Drug Delivery via the Transferrin Receptor-Mediated Endocytosis Pathway. *Pharmacol. Rev.* **2002**, *54*, 561.

For Table of Contents Only